

# Hydrogen bond dynamics at the glass transition

U. Buchenau\*

Forschungszentrum Jülich GmbH, Jülich Centre for Neutron Science (JCNS-1)  
and Institute for Complex Systems (ICS-1), 52425 Jülich, GERMANY

(Dated: May 17, 2021)

The glass transition in hydrogen-bonded glass formers differs from the glass transition in other glass formers. The Eshelby rearrangements of the highly viscous flow are superimposed by strongly asymmetric hydrogen bond rupture processes, responsible for the excess wing. Their influence on the shear relaxation spectrum is strong in glycerol and close to zero in PPE, reflecting the strength of the hydrogen bond contribution to the high frequency shear modulus. An appropriate modification of a recent theory of the highly viscous flow enables a quantitative common description of the relaxation spectra in shear, dielectrics, heat capacity and depolarized dynamic light scattering.

PACS numbers: 78.35.+c, 63.50.Lm

At the glass transition [1–4], hydrogen bonds [5, 6] have specific dynamics, always at the beginning and sometimes also at the end of the flow process: at long times, in the monoalcohols [7], the hydrogen bond decay is a Debye process, with a relaxation time much longer than the terminal shear relaxation time  $\tau_c$ , so the hydrogen bond connection memory can survive the breakdown of rigidity, similar to the case of polymers [8].

At short times, two peculiarities seem to appear exclusively in hydrogen-bonded glass formers, namely strongly asymmetric double-well potentials in the recoverable part of the flow relaxation [9, 10] and the excess wing at very short relaxation times [10–12]. Both features have very recently been shown to be absent in several non-hydrogen-bonding glass formers by combining mechanical data in the glass phase at many different frequencies from the literature [13].

The first clear evidence for strongly asymmetric double-well potentials in hydrogen-bonded substances appeared in an aging experiment [9]. An average asymmetry of  $3.8 k_B T_g$  is needed to explain the intensity rise of the strong secondary relaxation peak dielectric signal in tripropylene glycol immediately after the initial temperature jump.

The second proof for a strong asymmetry is the strong temperature dependence  $\exp(5T/T_g)$  of the excess wing measured in the glass phase of glycerol and other hydrogen bonded glass formers [10], explainable in terms of the asymmetry  $\Delta = 5k_B T_g$ , leading to the weakening factor  $1/\cosh(\Delta/2k_B T)^2 \approx \exp(5(T - 1.52T_g)/T_g)$  for  $T$  slightly below  $T_g$ .

The present paper argues that the process behind these strongly asymmetric double-well potentials is the reversible rupture of hydrogen bonds.

The breaking of hydrogen bonds has been intensely studied in liquid water and in the water shell of biomolecules [14, 15]. In liquid water at room temperature, a hydrogen bond between two water molecules has

two lifetimes, a short reversible one of 0.5 ps, after which it breaks, links to another water molecule, but then returns to its former state, and a longer irreversible one of 6.5 ps [14]. Both processes are visible in the dielectric spectrum of water [16, 17], the short time process accounting for about 10 % of the total decay. Obviously, this short time process is a rupture and re-formation of the hydrogen bond leading to a metastable energy minimum lying higher than the initial one, with a high back-jump probability, precisely the kind of process needed to understand the strongly asymmetric double-well potentials in the recoverable compliance of hydrogen-bonded glass formers.

The fact that the flow relaxation in all glass formers consists of a recoverable and an irreversible part is nowadays often overlooked [1–4], but has been established unambiguously long ago by the centennial shear relaxation work of Donald Plazek [18–21]. In the shear relaxation, the irreversible part is described by the viscosity  $\eta$ . The reversible part consists of a Kohlrausch tail  $t^\beta$  ( $t$  time,  $\beta$  Kohlrausch exponent) of the shear compliance at times shorter than the terminal relaxation time  $\tau_c$  of the viscous flow. Plazek favors the Andrade value  $\beta = 1/3$ . But his data do not establish  $\beta$  with high accuracy; more extensive investigations [22, 23] find a wide distribution of  $\beta$  values around 1/2.

A theoretical analysis of the reversible and irreversible shear transformation processes in the five-dimensional shear space [24–26] in terms of asymmetric double-well potentials, with the asymmetry determined exclusively by the different shear misfit of the inner Eshelby domain [27] or shear transformation zone [28, 29] in its two structural alternatives, leads to the relaxation time distribution in the barrier variable  $v = \ln(\tau/\tau_c)$

$$l_{irrev}(v) = \frac{1}{3\sqrt{2\pi}} \exp(v^2) \left( \ln(4\sqrt{2}) - v \right)^{3/2} \quad (1)$$

for the irreversible processes, with  $\tau_c = 8\eta/G$  ( $G$  short time shear modulus). Note that the spectrum has no Kohlrausch tail at short times. Its longest relaxation time is  $32\sqrt{2} \approx 45$  times longer than the Maxwell time. The spectrum is able to reproduce [26] a high quality

---

\*Electronic address: buchenau-juelich@t-online.de

measurement [30] of the terminal stage of the aging process in squalane, with  $\tau_c$  extrapolated from shear data in the liquid phase.

This irreversible process spectrum describes dynamic heat capacity data not only in a metallic glass, but also in three hydrogen bonding substances, the vacuum pump oil PPE, glycerol and propylene glycol [24, 25], with  $\tau_c$  determined from shear relaxation data of the same substances. Obviously, the additional asymmetric processes in these substances do not change the validity of eq. (1) for the irreversible flow processes. Since the theoretical analysis explains the irreversible processes quantitatively in terms of a continuation of the Eshelby processes of the Kohlrausch tail to relaxation times longer than  $\tau_c$ , this implies that there must be a basic Kohlrausch tail in the hydrogen-bonded substances identical to the one in other glass formers.

But what obviously happens is that the basic Kohlrausch tail relaxations combine with a reversible hydrogen bond rupture, creating a double well potential with a strong asymmetry. This effect is bound to become stronger as the Kohlrausch tail approaches from above barrier energies close to the breaking energy of the hydrogen bond [5, 6] of about 0.2 eV (this energy is about one third of the terminal flow barrier of about  $35 k_B T_g$ ). This is the physical reason for the excess wing.

How does this modify the basic Kohlrausch tail? The strengthening toward lower barriers adds a logarithmic curvature, so the tail has to be described in terms of a Kohlrausch barrier density  $\exp(\beta(v + f_{exc}v^2))$ , with a small excess wing parameter  $f_{exc}$ . The second necessary change has been already seen in the first attempt to fit hydrogen bonding spectra in terms of the theory [25]: because of the higher back-jump probability, one needs a higher Kohlrausch barrier density to achieve the viscous flow, describable in terms of a prefactor  $f_K > 1$  for the Kohlrausch tail. Together, these two effects modify the theoretical equation [26] into

$$l_K(v) = f_K(1 + 0.115\beta - 1.18\beta^2)F(v) \exp(\beta(v + f_{exc}v^2)). \quad (2)$$

Here  $F(v) \approx 1/(1 + \exp(1.19v))$  is the cutoff function of the Kohlrausch tail by the irreversible processes [26].

Having defined  $l_K(v)$ , one can calculate the complex shear compliance  $J(\omega)$  from

$$GJ(\omega) = 1 + \int_{-\infty}^{\infty} \frac{l_K(v)dv}{1 + i\omega\tau_c \exp(v)} - \frac{i}{\omega\tau_M}, \quad (3)$$

where  $\tau_M = \eta/G = \tau_c/8$  is the Maxwell time, and invert it to get  $G(\omega)$ .

Fig. 1 (a) shows the fit of the shear relaxation data [31] in glycerol at 196 K in terms of these equations, with the parameters compiled in Table I, demonstrating that the postulate of an additional slow mode [31] is not the only way to understand these data.

As pointed out in the theoretical paper [26], the simultaneous knowledge of irreversible and reversible relaxation processes from the shear data implies the knowledge

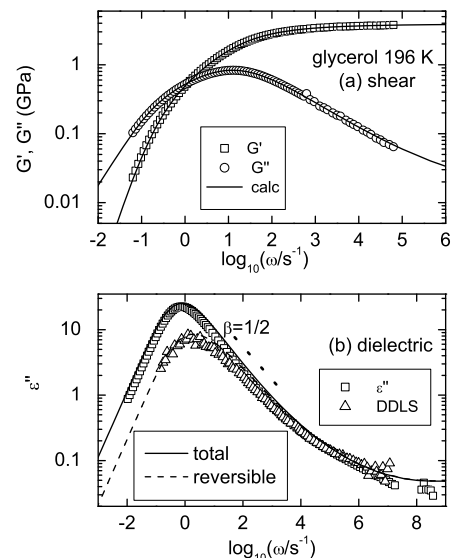


FIG. 1: (a) Measurement [31] of  $G(\omega)$  in glycerol, continuous lines calculated with the parameters in Table I (b) Fit of dielectric data [32] at the same temperature with the parameters in Table II. The dashed line is calculated without the irreversible processes, providing a very satisfactory description of the depolarized dynamic light scattering data [11].

subst.	$T$ K	$G$ GPa	$\eta$ GPas	$\beta$	$f_K$	$f_{exc}$	$GJ_0$
glycerol	196	3.93	1.80	0.65	5.95	0.014	11.2
propylene carbonate	159	1.47	0.523	0.51	1.51	0.009	4.26
PPE	250	1.09	0.725	0.48	1	0	3.03
propylene glycol	180	4.05	0.17	0.68	5.17	0.021	10.0

TABLE I: Parameters for the theoretical description of shear relaxation data (references see text) in the four hydrogen-bonded glass formers (PPE=5-polyphenylene ether).

of all relaxation processes of the substance, and enables one to predict what one should see in other relaxation techniques. The application of this concept to dielectric and adiabatic compressibility data in non-hydrogen-bonded glass formers revealed that the scheme works very well, but the dielectric and compressibility signals required the multiplication of the total spectrum with  $\exp(-\tau/\tau_t)$ , where  $\tau_t$  is a terminal time shorter than  $\tau_c$ , showing that the dielectric polarizability and the adiabatic compressibility equilibrate earlier than the terminal shear relaxation time.

In the application of the scheme to dielectric and depolarized dynamic light scattering in hydrogen bonded substances, one must multiply also the irreversible contribution of eq. (1) with  $f_K$ , because otherwise there is a discontinuity in the coupling constant at  $\tau_c$ . The resulting barrier density is

$$l_{tot}(v) = l_0(8f_K l_{irrev}(v) + l_K(v)) \exp(-\exp(v)/\tau_t), \quad (4)$$

with the appropriate normalization factor  $l_0$ .

Fig. 1 (b) shows that one can describe the dielectric spectrum at the same temperature [32] and depolarized dynamic light scattering data at 190 K [11], shifted to 196 K with the appropriate shift factor, with this recipe. However, one must adapt the excess wing parameter  $f_{exc}$ , which is a bit larger in the dielectric data. As a consequence, one must also adapt  $\beta$  to a slightly higher value, because the slope of the Kohlrausch tail at  $\tau_c$  contains a small negative component from the diminishing influence of hydrogen bonds toward higher barriers. The four parameters  $\Delta\epsilon$  (the difference between the dielectric susceptibilities at very low and very high frequency),  $f_{exc}$ ,  $\tau_t/\tau_c$  and  $\beta$  for the dielectric data are listed in Table II.

subst.	$T$ K	$\Delta\epsilon$	$\beta$	$f_{exc}$	$\tau_t/\tau_c$
glycerol	196	62.7	0.71	0.017	0.108
propylene carbonate	159	76.5	0.56	0.012	6.02
PPE	250	1.9	0.68	0.017	0.099
propylene glycol	180	64.4	0.60	0.017	2578

TABLE II: Parameters for the theoretical description of dielectric relaxation data (references see text) in the four hydrogen-bonded glass formers.

Fig. 1 (b) shows also, as a dashed line, the calculated dielectric signal without the irreversible processes, which describes the shifted depolarized dynamic light scattering data [11] very well. This can be understood: The reversible hydrogen bond jumps are large angle jumps of 50 to 60 degrees [14], while the irreversible processes according to NMR evidence [33] lead essentially to a small angle orientational diffusion of the whole molecule, to which the hydrogen bond belongs. This is a different kind of motion, which obviously has a much smaller depolarized dynamic scattering signal.

Glycerol with its three strong oxygen hydrogen bonds per molecule has a much higher shear modulus than propylene carbonate, where the oxygen atoms do not have a hydrogen atom of their own, but link to the hydrogens bonded to carbon atoms. As a consequence, the deviation of the parameter  $f_K$  from 1 in Table I of propylene carbonate is about a factor of ten smaller than the one of glycerol, and its shear modulus is not much higher than the 1 GPa of van-der-Waals bonded molecular glass formers [25]. But otherwise, the results of the same analysis of propylene carbonate data [34] shown in Fig. 2 (a) and (b) and tabulated in Table I and II are very similar.

PPE has even weaker hydrogen bonds, so weak that one gets a perfect fit of the shear data [35] in terms of the original model with only the three parameters  $G$ ,  $\eta$  and  $\beta$  in Table I, taken over from [26]. But the former fit of the dielectric data [26] improves markedly with the parameters of Table II, as demonstrated in Fig. 3. The excess wing parameter is about the same as in the other three substances and  $\beta$  changes strongly, showing that the dielectric signal has a strong hydrogen bond component which is not visible in the shear data.

The last example, propylene glycol, shows that it can

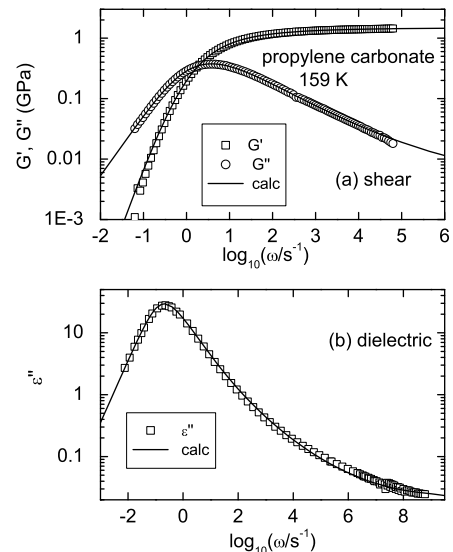


FIG. 2: (a) Measurement [34] of  $G(\omega)$  in propylene carbonate at 159 K, continuous lines calculated with the parameters in Table I (b) Fit of dielectric data [34] at the same temperature in the same cryostat with the parameters in Table II.

also be the other way round. The hydrogen bond component is actually stronger in the shear data [36] than in the dielectric data [37], where one finds a smaller  $f_{exc}$  and a smaller  $\beta$  than in the shear data. In this case, one does not really need  $\tau_t$ ; the dielectric relaxation terminates at the value calculated from the shear data.

Table I compiles the parameters for the four substances, including in the last row the total recoverable compliance  $GJ_0$ , which in glycerol is nearly a factor of four higher than in normal glass formers, showing that one needs much more recoverable processes to start the viscous flow, because of the strong back-jump tendency of the hydrogen bonds. In all four cases, the shear analysis was done over the entire temperature range of the measurements, to look for a possible temperature dependence of the parameters.  $f_K$  and  $f_{exc}$  were found to be temperature-independent within experimental accuracy

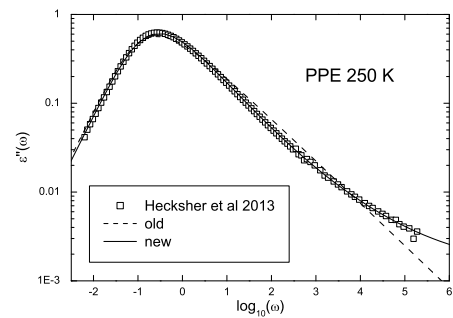


FIG. 3: (Old [26] (dashed line) and new (continuous line, parameters Table II) calculations for dielectric data in PPE at 250 K [35].

in the three cases were they were not fixed. For glycerol, the temperature-dependent shear moduli agreed within a few percent with those of a transverse wave Brillouin scattering determination [38], showing the high quality of both measurements.

Though one has to invoke an additional mechanism, the possibility to obtain good fits of high quality shear data in hydrogen bonding substances with the two additional parameters  $f_K$  for the strength of the hydrogen bond influence and  $f_{exc}$  for the excess wing curvature supports the validity of the general theory of the highly viscous flow [26].

To summarize, one can understand the shear relax-

ation of hydrogen-bonded undercooled liquids close to their glass transition in a recent theory of the highly viscous flow by taking the influence of highly asymmetric reversible hydrogen bond ruptures, well studied in water, into account. The hydrogen bond ruptures make the Kohlrausch tail double-well potentials strongly asymmetric and give rise to the excess wing, absent in non-hydrogen-bonded glass formers. One can describe shear, dielectric, depolarized dynamic light scattering and dynamic specific heat data consistently within the extended theory, noting that one sees only reversible processes in the depolarized dynamic light scattering data.

- 
- [1] A. Cavagna, Phys. Rep. **476**, 51 (2009)
  - [2] L. Berthier and G. Biroli, Rev. Mod. Phys. **83**, 587 (2011)
  - [3] C. P. Royall and S. R. Williams, Phys. Rep. **560**, 1 (2015)
  - [4] L. Berthier, J. Chem. Phys. **150**, 160902 (2019)
  - [5] Th. Steiner, Angew. Chem. Int. Ed. **41**, 48 (2002)
  - [6] V. David, N. Grinberg, and S. C. Moldoveanu, in *Advances in Chromotography Vol. 54* (Eds: E. Gruschka, N. Grinberg), CRC, Boca Raton 2018, chap. 3
  - [7] R. Böhmer, C. Gainaru, and R. Richert, Phys. Rep. **545**, 125 (2014)
  - [8] A. L. Agapov, V. N. Novikov, T. Hong, F. Fan, and A. P. Sokolov, Macromolecules **51**, 4874 (2018)
  - [9] J. C. Dyre and N. B. Olsen, Phys. Rev. Lett. **91**, 155703 (2003)
  - [10] C. Gainaru, R. Böhmer, R. Kahlau, and E. Rössler, Phys. Rev. B **82**, 104205 (2010)
  - [11] J. Ph. Gabriel, P. Zourchang, F. Pabst, A. Helbling, P. Weigl, T. Böhmer, and Th. Blochowicz, Phys. Chem. Chem. Phys. **22**, 11644 (2020)
  - [12] F. Pabst, J. Ph. Gabriel, T. Böhmer, P. Weigl, A. Helbling, T. Richter, P. Zourchang, Th. Walther, and Th. Blochowicz, J. Phys. Chem. Lett. **12**, 14 (2021)
  - [13] U. Buchenau, G. D'Angelo, G. Carini, X. Liu, and M. A. Ramos, arXiv:2012.10139
  - [14] B. Bagchi, Chem. Rev. **105**, 3197 (2003)
  - [15] D. Laage and J. T. Hynes, Science **311**, 832 (2006)
  - [16] J. B. Hasted, S. K. Husain, F. A. M. Frescura, and R. Birch, Chem. Phys. Lett. **118**, 622 (1985)
  - [17] W. J. Ellison, K. Lamakaouchi, and J.-M. Moreau, J. Mol. Liq. **68**, 171 (1996)
  - [18] D. J. Plazek, J. Phys. Chem. **69**, 3480 (1965)
  - [19] D. J. Plazek and J. H. Magill, J. Chem. Phys. **45**, 3038 (1966)
  - [20] D. J. Plazek, C. A. Bero and I.-C. Chay, J. Non-Cryst. Solids **172-174**, 181 (1994)
  - [21] C. M. Roland, P. G. Santangelo, D. J. Plazek, and K. M. Bernatz, J. Chem. Phys. **111**, 9337 (1999)
  - [22] R. Böhmer, K. L. Ngai, C. A. Angell and D. J. Plazek, J. Phys. Chem. **99**, 4201 (1993)
  - [23] A. I. Nielsen, T. Christensen, B. Jakobsen, K. Niss, N. B. Olsen, R. Richert, and J. C. Dyre, J. Chem. Phys. **130**, 154508 (2009)
  - [24] U. Buchenau, J. Chem. Phys. **148**, 064502 (2018)
  - [25] U. Buchenau, J. Chem. Phys. **149**, 044508 (2018)
  - [26] U. Buchenau, arXiv:2003.07246
  - [27] J. D. Eshelby, Proc. Roy. Soc. **A241**, 376 (1957)
  - [28] M. L. Falk and J. S. Langer, Phys. Rev. E **57**, 7192 (1998)
  - [29] W. L. Johnson and K. Samwer, Phys. Rev. Lett. **95**, 195501 (2005)
  - [30] K. Niss, J. C. Dyre, and T. Hecksher, J. Chem. Phys. **152**, 041103 (2020)
  - [31] M. H. Jensen, C. Gainaru, C. Alba-Simionesco, T. Hecksher, and K. Niss, Phys. Chem. Chem. Phys. **20**, 1716 (2018)
  - [32] S. Adichtchev, T. Blochowicz, C. Tschirwitz, V. N. Novikov and E. A. Rössler, Phys. Rev. E **68**, 011504 (2003)
  - [33] G. Diezemann, R. Böhmer, G. Hinze, and H. Sillescu, J. Non-Cryst. Solids **235-237**, 121 (1998)
  - [34] C. Gainaru, T. Hecksher, N. B. Olsen, R. Böhmer, and J. C. Dyre, J. Chem. Phys. **137**, 064508 (2012)
  - [35] T. Hecksher, N. B. Olsen, K. A. Nelson, J. C. Dyre and T. Christensen, J. Chem. Phys. **138**, 12A543 (2013)
  - [36] C. Maggi, B. Jakobsen, T. Christensen, N. B. Olsen and J. C. Dyre, J. Phys. Chem. B **112**, 16320 (2008)
  - [37] C. Leon, K. L. Ngai, and C. M. Roland, J. Chem. Phys. **110**, 11585 (1999)
  - [38] F. Scarponi, L. Comez, D. Fioretto, and L. Palmieri, Phys. Rev. B **70**, 054203 (2004)